Available online at www.sciencedirect.com
ScienceDirect
Journal of Sound and Vibration 310 (2008) 966–984
JOURNAL OF SOUND AND VIBRATION
www.elsevier.com/locate/jsvi

Nonlinear free and forced vibration analysis of thin circular functionally graded plates

A. Allahverdizadeh*, M.H. Naei, M. Nikkhah Bahrami

School of Mechanical Engineering, University of Tehran, Tehran, Iran

Received 22 August 2006; received in revised form 16 August 2007; accepted 16 August 2007
Available online 21 September 2007

Abstract

In this paper, a semi-analytical approach for nonlinear free and forced axisymmetric vibration of a thin circular functionally graded plate is developed. The plate thickness is constant. Functionally graded material (FGM) properties vary through the thickness of the plate. For harmonic vibrations, by using assumed-time-mode method and Kantorovich time averaging technique, the governing equations are solved. Steady-state free and forced vibration analysis is investigated in detail and corresponding results at uniform ambient temperature are illustrated. Some of these results in special cases are verified by comparing with those in the literature. The results show that the free vibration frequencies are dependent on vibration amplitudes, and that the volume fraction index has a significant influence on the nonlinear response characteristics of the plate.

1. Introduction

Thin plate structures are encountered in various modern engineering problems and they are often subjected to sever dynamic loading. This may result in large vibration amplitudes of these structures. When the amplitude of vibration is of the same order of the plate thickness, a significant geometrical nonlinearity is induced and the linear model is not sufficient to predict the behavior of the plate such as jump phenomenon; so the dynamic analog of the von-Karman equations, as the nonlinear equations of motion for thin plates, are used widely.

Huang and Sandman [1] and Huang and Al-Khattat [2], investigated the nonlinear free and forced vibrations of circular and annular plates with various boundary conditions. The von-Karman equations and the Kantorovich method were used, and numerical results were obtained by solving numerically a two-point boundary value problem. Haterbouch and Benamar [3,4] presented a more complete study for the effects of large vibration amplitudes on the axisymmetric mode shapes and natural frequencies of clamped thin isotropic circular plates.

Layered composite materials, due to their thermal and mechanical merits compared to single composed materials, have been widely used for a variety of engineering applications. However, owing to the sharp

*Corresponding author. Tel.: +98 21 88005677; fax: +98 21 88013029.
E-mail address: allahverdizadeh@gmail.com (A. Allahverdizadeh).

0022-460X/$ - see front matter © 2007 Elsevier Ltd. All rights reserved.
doi:10.1016/j.jsv.2007.08.011

Nomenclature

a	radius of circular plate
c	ceramic, non-dimensional radius of the solid circular plate
E	Young's modulus
F, G	non-dimensional shape functions
h	plate thickness
m	metal
M_r, M_θ	bending moments per unit length
n	volume fraction index
N_r, N_θ	membrane forces per unit length
$P(r,t)$	uniformly distributed lateral loading intensity
$q(r^*,\tau)$	non-dimensional lateral loading intensity
Q_r	shearing force per unit length
r, θ, z	cylindrical coordinates
t	time variable
u, w	radial and transverse displacements of the middle plane, respectively
u_r, u_z	displacements along r and z directions, respectively
V	volume fraction
ε_r, ε_θ	normal strains along the r and θ directions
v	Poisson's ratio
ρ	mass density
σ_r, σ_θ	radial and circumferential total stresses
τ	dimensionless time variable
ϕ	non-dimensional stress function
$\psi(r,t)$	stress function
ω_{bi}	non-dimensional linear natural frequency
Ω	linear natural frequency
*	star exponent indicates non-dimensional parameters

discontinuity in the material properties at interfaces between two different materials, there may exist stress concentrations which result in sever material failure. To remedy such defects, functionally graded materials (FGMs) have been proposed. FGMs are spatial composites within which material properties vary continuously and inhomogeneously. The advantage of using these materials is that they can survive the high thermal gradient environment while maintaining their structural integrity. Typically, FGMs are made from mixture of two or more materials that are appropriate to achieve the desired objective. FGMs properties vary continuously from one interface to the other. Those are achieved by gradually varying volume fraction of constituent materials. FGMs have different applications especially for aircrafts, space vehicles, automobile, defense industries, electronics, biomedical sectors and other engineering structures.

Many studies for vibration of functionally graded plates are available in the literature. For dynamic behavior of FGMs, Praveen and Reddy [5] conducted the nonlinear transient thermoelastic analysis of functionally graded ceramic-metal plates using finite element method. Yang and Shen [6] deal with the dynamic response of initially stressed FGM rectangular thin plates subjected to impulsive loads. Effects of volume fraction index, foundation stiffness, plate aspect ratio, the shape and duration of impulsive load on the dynamic response of FGM plates were studied in this work. They [7] also considered the vibration characteristics and transient response of shear-deformable FGM plates made of temperature-dependent materials in thermal environments. Differential quadrature technique, Galerkin approach, and the modal superposition method are used to determine the transient response of the plate subjected to lateral dynamic loads. Huang and Shen [8] discussed the nonlinear vibration and dynamic response of functionally graded plates in a thermal environment by using improved perturbation technique. The results reveal that the temperature field and volume fraction distribution have significant effect on the nonlinear vibration and dynamic response of the simply supported rectangular plate with no in-plane displacements. Reddy and Cheng [9] studied the harmonic vibration problem of functionally graded plates by means of a three-dimensional asymptotic theory formulated in terms of transfer matrix. Woo and Meguid [10] investigated the nonlinear analysis of functionally graded plates and shallow shells. An analytical solution has been provided for the coupled large deflection of plates and shallow shells under mechanical load and temperature field, and the solution has been obtained in terms of Fourier series. Woo et al. [11] derived an analytical solution for the nonlinear free vibration behavior of thin rectangular functionally graded plates. Kitipornchai et al. [12] presented a semi-analytical solution for nonlinear vibration of laminated FGM plates with geometric imperfections and showed that the vibration frequencies are very much dependent on the vibration amplitude

and the imperfection mode. They [13] also studied the random vibration of the functionally graded laminates with third-order shear deformation plate theory and general boundary conditions in thermal environments. Yang et al. [14] presented a large amplitude vibration analysis of pre-stressed FGM laminated plates that are composed of a shear deformable functionally graded layer and two surface-mounted piezoelectric actuator layers.

In this paper, the problem of large amplitude axisymmetric vibration of a thin circular functionally graded plate is formulated in terms of von-Karman's dynamic equations. FGM properties vary through the constant thickness of the plate. For harmonic vibrations, the time variable is eliminated by employing the Kantorovich averaging method. Therefore the basic governing equations for the problem are reduced to a pair of ordinary differential equations, which form a nonlinear boundary value problem. A numerical study of these governing equations at uniform ambient temperature is accomplished by shooting and Runge–Kutta integration methods.

2. Theoretical formulations

Modern light-weight designs often require that thin-plate structures be able to withstand large amplitude of vibration when they are subjected to dynamic loading conditions. If the amplitude of motion is of the same order of magnitude as the thickness of the plate, then the mathematical description of the motion must be extended from classical linear plate theory to include deformation of the middle plane. For proper design, the influence of this membrane effect upon the strength and responsiveness of the plate should be established. In the development of a suitable theory, geometric nonlinearities arise in a coupling of membrane and bending theories for thin plates. There are several theories dealing with plates. For thin plates, von-Karman's large deflection theory [15,16] provides a good approximation and is usually applied [4]. Due to the complex nature of the resulting governing equations, it appears that the only present means of solution to large amplitude plate vibration problems is by approximate methods of various types.

2.1. FGM properties

Consider a FGM plate of constant thickness h and radius a, which is made from a mixture of ceramic and metal and the composition varies from the top to the bottom surface, i.e. the top surface ($z = h/2$) of the plate is ceramic-rich whereas the bottom surface ($z = -h/2$) is metal-rich. In such a way, an arbitrary material property P (e.g., Young's modulus E, and mass density ρ) of the functionally graded plate is assumed to vary through the thickness of the plate, as a function of the volume fraction and properties of the constituent materials as

$$P = P_t V_c + P_b V_m, \tag{1}$$

where P_t and P_b stand for the temperature-dependent properties of the top and bottom surfaces of the plate and may be expressed as a function of temperature [17] as

$$P = P_0(P_{-1}T^{-1} + 1 + P_1 T + P_2 T^2 + P_3 T^3). \tag{2}$$

In which P_0, P_{-1}, P_1, P_2, and P_3 are the coefficients of temperature T (K), and are unique to the constituent materials. In Table 1, typical values for silicon nitride and stainless steel are listed [18]. V_c and V_m are the ceramic and metal volume fractions and are related by

$$V_c + V_m = 1. \tag{3}$$

For a plate with an uniform thickness h and a reference surface at its middle surface, the volume fraction V_c follows a simple power law as

$$V_c(z) = \left(\frac{2z + h}{2h}\right)^n. \tag{4}$$

Volume fraction index n dictates the material variation profile across the plate thickness. It is assumed that the effective Young's modulus E depends on temperature, whereas the mass density ρ is independent from the

Table 1
Temperature-dependent coefficients of material properties [18]

Property	Material	P_{-1}	P_0	P_1	P_2	P_3
E (GPa)	Si_3N_4	0	384.43e9	−3.070e−4	2.160e−7	−8.946e−11
	SUS304	0	201.04e9	3.079e−4	−6.534e−7	0
ρ (kg/m^3)	Si_3N_4	0	2370	0	0	0
	SUS304	0	8166	0	0	0
v	Si_3N_4	–	0.2400	–	–	–
	SUS304	–	0.3177	–	–	–

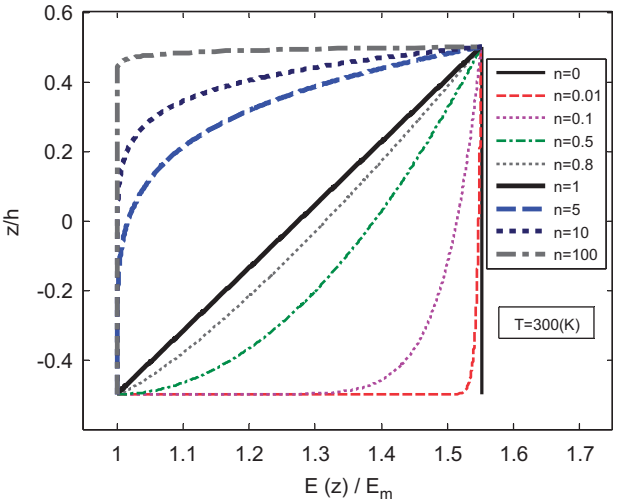

Fig. 1. Variation of the dimensionless Young's modulus through the dimensionless thickness.

temperature. Poisson's ratio v is considered to be constant. From Eqs. (1)–(4), one has [19,20]

$$P(z) = (P_c - P_m)\left(\frac{2z+h}{2h}\right)^n + P_m. \tag{5}$$

In what follows, a metal, stainless steel (SUS304) and ceramics, silicon nitride (Si_3N_4) system of FGM is considered. The temperature-dependent material properties are given in Table 1 and are calculated by using Eq. (5).

Fig. 1 shows the variation of the dimensionless Young's modulus $E(z)/E_m$ of the functionally graded plate through the dimensionless thickness z/h with different values of volume fraction index n. If $n = 0$ then the plate reduces to a pure ceramic plate. As the volume fraction index n increases, the ceramic volume fraction decreases. It is seen that in a same z/h, by increasing n, the dimensionless Young's modulus decreases. Fig. 2 indicates the variation of the dimensionless mass density $\rho(z)/\rho_m$ with the dimensionless thickness z/h of the plate for different values of n. We suppose that the mass density is independent of temperature. The non-dimensional mass density increases from ρ_c/ρ_m at $z = h/2$ to 1 at $z = -h/2$. At z closer to $z = -h/2$, the rate of decrease of $\rho(z)/\rho_m$ for $n<1$ is high compared to $n>1$. By increasing n with the same z/h, it is observed that $\rho(z)/\rho_m$ increases.

2.2. Governing equations

Consider a thin circular FGM plate subjected to axisymmetric transverse load and located in its initially undeformed configuration by cylindrical coordinates r, θ and z. The r-coordinate direction is radially outward

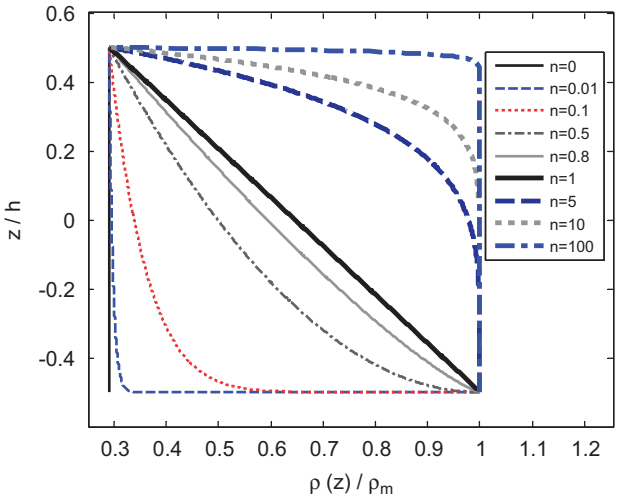

Fig. 2. Variation of the dimensionless mass density through the dimensionless thickness.

from the center, the z-coordinate is along the thickness, and the θ-coordinate is directed along a circumference of the plate. The disk has uniform thickness h and it is bounded by the planes $z = \pm h/2$ and the cylinder $r = a$. The plate is excited in a manner which produces large amplitude vibration. The position of a point inside the disk is defined by the radial coordinate r and the transverse coordinate z. The radial displacement u_r and the transverse displacement u_z show the displacement of the point. These displacements are expressed in terms of the displacements for a point on the middle surface of the disk using the Kirchhoff plate theory [21]:

$$u_r(r, z, t) = u(r, t) - zw(r, t)_{,r}, \tag{6}$$

$$u_z(r, z, t) = w(r, t), \tag{7}$$

where $u(r, t)$ and $w(r, t)$ are the radial and transverse displacements of the point on the middle surface of the plate, respectively.

In the following, governing equations for the ensuing motion are derived. The underlying assumptions are the followings. Firstly, normals of the middle plane before bending remain straight and normal to the middle plane after bending. Secondly, slopes produced by flexure are moderately large, but small in comparison with unity. Thirdly, normal stresses σ_z are small compared with other stress components and may be neglected in the stress–strain relations. Finally, the loads and deflections of the plate are symmetrical with respect to the z-axis.

In accordance with these assumptions, the strains at any level z from the neutral plane are obtained by substituting the classical plate deformation kinematics relations in the nonlinear strain-displacement relations as [22–24]

$$\varepsilon_r = u_{,r} + \tfrac{1}{2}(w_{,r})^2 - zw_{,rr}, \tag{8}$$

$$\varepsilon_\theta = \frac{u}{r} - z\frac{1}{r}w_{,r}, \tag{9}$$

where ε_r and ε_θ are the normal strains along the r and θ directions. In terms of Hooke's laws, the radial and circumferential total stresses are given by

$$\sigma_r = \frac{E(z, T)}{1 - \nu}\left[\frac{1}{1 + \nu}(\varepsilon_r + \nu\varepsilon_\theta)\right], \tag{10}$$

$$\sigma_\theta = \frac{E(z, T)}{1 - \nu}\left[\frac{1}{1 + \nu}(\varepsilon_\theta + \nu\varepsilon_r)\right], \tag{11}$$

where

$$E(z,T) = E_{cm}(T)\left(\frac{2z+h}{2h}\right)^n + E_m(T), \quad E_{cm} = E_c - E_m. \tag{12}$$

The membrane forces may be

$$(N_r, N_\theta) = \int_{-h/2}^{h/2} (\sigma_r, \sigma_\theta)\,\mathrm{d}z, \tag{13}$$

$$N_r = \frac{h}{1-v^2}\left[A\left\{u_{,r} + \frac{1}{2}(w_{,r})^2 + v\frac{u}{r}\right\} - Bh\left\{w_{,rr} + v\frac{1}{r}w_{,r}\right\}\right], \tag{14}$$

$$N_\theta = \frac{h}{1-v^2}\left[A\left\{\frac{u}{r} + v\left(u_{,r} + \frac{1}{2}(w_{,r})^2\right)\right\} - Bh\left\{\frac{1}{r}w_{,r} + vw_{,rr}\right\}\right], \tag{15}$$

where A and B are defined as

$$A = \left(E_m + \frac{E_{cm}}{n+1}\right), \tag{16}$$

$$B = \frac{nE_{cm}}{2(n+1)(n+2)}. \tag{17}$$

And the bending moments become

$$(M_r, M_\theta) = \int_{-h/2}^{h/2} (\sigma_r, \sigma_\theta) z\,\mathrm{d}z, \tag{18}$$

$$M_r = \frac{h^3}{1-v^2}\left[-R\left\{w_{,rr} + v\frac{1}{r}w_{,r}\right\} + \frac{B}{h}\left\{u_{,r} + \frac{1}{2}(w_{,r})^2 + v\frac{u}{r}\right\}\right], \tag{19}$$

$$M_\theta = \frac{h^3}{1-v^2}\left[-R\left\{\frac{1}{r}w_{,r} + vw_{,rr}\right\} + \frac{B}{h}\left\{\frac{u}{r} + v\left(u_{,r} + \frac{1}{2}(w_{,r})^2\right)\right\}\right], \tag{20}$$

where

$$R = \frac{E_m}{12} + \frac{(n^2+n+2)}{4(n+1)(n+2)(n+3)}E_{cm}. \tag{21}$$

For homogeneous materials, the above relations are identical with Refs. [16,24]. By writing the equilibrium equation for the forces projected in the radial direction, and neglecting the longitudinal inertia, the result is [16,24]

$$N_{r,r} + \frac{1}{r}(N_r - N_\theta) = 0. \tag{22}$$

Since the principal vibrations take place in the direction perpendicular to the middle plane, it is reasonable to neglect the longitudinal inertia. By eliminating the radial displacement function $u(r,t)$ from Eqs. (14) and (15), the compatibility equation is obtained with the aid of Eq. (22)

$$(N_r + N_\theta)_{,r} = \frac{-hA}{2r}(w_{,r})^2 \tag{23}$$

when the stress function $\psi(r,t)$, and the corresponding relations

$$N_r = \frac{\psi}{r}, \quad N_\theta = \psi_{,r} \tag{24}$$

which satisfy (22) exactly, are introduced into Eq. (23), the result is

$$\psi_{,rr}+\frac{1}{r}\psi_{,r}-\frac{\psi}{r^2}=\frac{-hA}{2r}(w_{,r})^2. \tag{25}$$

The equation of the moment equilibrium about a circumferential tangent is

$$M_{r,r}+\frac{M_r-M_\theta}{r}=Q_r, \tag{26}$$

where Q_r is the shearing force per unit length. By applying d'Alembert's principle, dynamic equilibrium of the transverse forces, which act on an annular element, requires that

$$(rQ_r)_{,r}+(rN_rw_{,r})_{,r}+rP(r,t)=h\left(\frac{\rho_{cm}}{n+1}+\rho_m\right)rw_{,tt},\quad \rho_{cm}=\rho_c-\rho_m, \tag{27}$$

where $P(r,t)$ is the uniformly distributed lateral loading intensity. Combining Eqs. (19), (20), (24), (26) and (27) one may obtain the equation

$$\begin{aligned}&-\left(\frac{h^3B^2}{A(1-v^2)}-\frac{h^3R}{1-v^2}\right)(\nabla^4w)-\frac{1}{r}(\psi w_{,r})_{,r}+h\left(\frac{\rho_{cm}}{n+1}+\rho_m\right)w_{,tt}\\&-\frac{h^2B}{1-v^2}\left[\frac{r}{hA}(\psi_{,rrrr})+\frac{5-v}{hA}(\psi_{,rrr})+\frac{3-2v}{rhA}(\psi_{,rr})+\frac{v}{r^2hA}(\psi_{,r})-\frac{v}{r^3hA}(\psi)\right]\\&-\frac{h^2B}{1-v^2}\left[(w_{,r})(w_{,rrr})+(w_{,rr})^2+\frac{2-v}{r}(w_{,r})(w_{,rr})\right]=P(r,t),\end{aligned} \tag{28}$$

where

$$\nabla^4w=w_{,rrrr}+\frac{2}{r}w_{,rrr}-\frac{1}{r^2}w_{,rr}+\frac{1}{r^3}w_{,r}. \tag{29}$$

Eqs. (25) and (28) are dynamic forms of von-Karman's equations, where the longitudinal and rotary inertias are neglected. Together, they govern the finite-amplitude axisymmetric vibration of a thin circular plate. By introducing dimensionless variables as

$$\begin{aligned}&r^*=r/a,h^*=h/a,u^*=u/a,w^*=w/a,\quad \rho^*_{cm}=\rho_{cm}/\rho_m,\\&\phi=\psi/(a^2E_m),\quad \tau=1/a\sqrt{E_m/\rho_m}t,\quad \Omega^*=a\sqrt{\rho_m/E_m}\Omega,\quad q(r^*,\tau)=P(r,t)/E_m\end{aligned} \tag{30}$$

and

$$A^*=A/E_m,\quad B^*=B/E_m,\quad R^*=R/E_m \tag{31}$$

the governing equations can now be written in non-dimensional form. In the following equations we neglect $()^*$:

$$\phi_{,rr}+\frac{1}{r}\phi_{,r}-\frac{\phi}{r^2}=-\frac{hA}{2r}(w_{,r})^2, \tag{32}$$

$$\begin{aligned}&-\left(\frac{h^3B^2}{A(1-v^2)}-\frac{h^3R}{1-v^2}\right)(\nabla^4w)-\frac{1}{r}(\phi w_{,r})_{,r}+h\left(\frac{\rho_{cm}}{n+1}+1\right)w_{,\tau\tau}\\&-\frac{h^2B}{1-v^2}\left[\frac{r}{hA}(\phi_{,rrrr})+\frac{5-v}{hA}(\phi_{,rrr})+\frac{3-2v}{rhA}(\phi_{,rr})+\frac{v}{r^2hA}(\phi_{,r})-\frac{v}{r^3hA}(\phi)\right]\\&-\frac{h^2B}{1-v^2}\left[(w_{,r})(w_{,rrr})+(w_{,rr})^2+\frac{2-v}{r}(w_{,r})(w_{,rr})\right]=q(r,\tau).\end{aligned} \tag{33}$$

These governing differential equations are complicated by the obvious nonlinear coupling of membrane and bending theories for thin plates.

In order to complete the formulation of the problem, the governing Eqs. (32) and (33) must be accompanied by a set of boundary conditions at the outer boundary for all dimensionless time τ. The boundary conditions

for $w(r,\tau)$ depend upon the degree of transverse constraint and those for $\phi(r,\tau)$ depend upon the degree of radial constraint. For a circular plate with clamped immovable edge, the following conditions are presented. The boundary conditions at center are as

$$w_{,r} = 0, \quad u = 0. \tag{34}$$

By using Eqs. (14) and (15) and also by substituting the dimensionless variables, the non-dimensional radial displacement function $u(r,\tau)$ may be:

$$u = \frac{ar}{hA}\phi_{,r} - \frac{va}{hA}\phi + \frac{ahB}{A}w_{,r}. \tag{35}$$

The plate edge is clamped and immovable in r direction, thus requires zero radial displacement; so the boundary conditions at $r = 1$ can be expressed as

$$w = 0, \quad w_{,r} = 0, \quad u = 0. \tag{36}$$

3. Method of solution

An exact solution of the differential Eqs. (32) and (33), which satisfies boundary conditions of the form (34)–(36), is at present unknown. The standard Fourier analysis used in linear vibration problems cannot be applied in an exact sense due to nonlinear character of the differential equations which causes a coupling of vibration modes. Consequently, the analysis and solution of the problem must be completed in some approximate manner. In most of the studies carried out on large vibration amplitudes of circular plates, the common approach has been to use an assumed space or time mode. In the assumed time function method, a simple harmonic function in time is assumed and is then eliminated from the equation of motion using the Kantorovich averaging procedure. The resulting nonlinear spatial boundary value problem is solved numerically. This technique has been used with von-Karman equations in Refs. [1,2,25–28]. Shooting method or trial and error method [29,30] was employed to get a numerical solution of the nonlinear two point boundary-value problem.

3.1. Kantorovich averaging method

The first simplification is imposed by taking the time varying loading intensity to be the form,

$$q(r,\tau) = Q(r)\sin\,\Omega\tau \tag{37}$$

with the plate being subjected to an uniformly distributed sinusoidal loading, it is assumed that the steady-state response can be closely approximated by the expressions

$$w(r,\tau) = G(r)\sin\,\Omega\tau, \tag{38}$$

$$\phi(r,\tau) = F(r)(\sin\,\Omega\tau)^2, \tag{39}$$

where $F(r)$ and $G(r)$ are undetermined shape functions of vibration. The assumption $\phi(r,\tau)$ follows from Eq. (38) and the supposition that the resulting membrane stresses should be independent of the up or down position of the plate. Substituting Eqs. (38) and (39) into the governing Eq. (32), one finds,

$$F_{,rr} + \frac{1}{r}F_{,r} - \frac{F}{r^2} = -\frac{hA}{2r}(G_{,r})^2. \tag{40}$$

Since expressions (37)–(39) cannot satisfy Eq. (33) for all τ, the following integral is employed to obtain a governing equation which closely approximate Eq. (33) within the limits of the assumed form of motion and loading as given in Eqs. (37)–(39), respectively,

$$I = \int_R^1 I_1 \delta w(2\pi r\,\mathrm{d}r), \tag{41}$$

$$I_1 = -\left(\frac{h^3B^2}{A(1-v^2)}-\frac{h^3R}{1-v^2}\right)(\nabla^4 w)-\frac{1}{r}(\phi w_{,r})_{,r}+h\left(\frac{\rho_{cm}}{n+1}+1\right)w_{,\tau\tau}$$
$$-\frac{h^2B}{1-v^2}\left[\frac{r}{hA}(\phi_{,rrrr})+\frac{5-v}{hA}(\phi_{,rrr})+\frac{3-2v}{rhA}(\phi_{,rr})+\frac{v}{r^2hA}(\phi_{,r})-\frac{v}{r^3hA}(\phi)\right]$$
$$-\frac{h^2B}{1-v^2}\left[(w_{,r})(w_{,rrr})+(w_{,rr})^2+\frac{2-v}{r}(w_{,r})(w_{,rr})\right]-q(r,\tau). \tag{42}$$

For any instant of dimensionless time τ, the relation (41) is equal to the virtual work of all the transverse forces as they move through a virtual displacement $\delta w(r,\tau)$. Equating the average virtual work over one period oscillation to zero,

$$I_A=\int_0^{2\pi/\Omega} I\,\mathrm{d}\tau=0 \tag{43}$$

yields

$$-\left(\frac{h^3B^2}{A(1-v^2)}-\frac{h^3R}{1-v^2}\right)(\nabla^4 G)-\frac{3}{4r}(FG_{,r})_{,r}-h\left(\frac{\rho_{cm}}{n+1}+1\right)\Omega^2G-\frac{h^2B}{1-v^2}(G_{,rr})^2=Q. \tag{44}$$

Thus, the assumed harmonic vibrations become governed by the pair of nonlinear, ordinary differential Eqs. (40) and (44). These equations along with a set of boundary conditions compose a nonlinear two-point boundary value problem which describes the harmonic response of a circular plate undergoing finite amplitude oscillations. Solving this nonlinear boundary-value problem completes the analysis and reveals the salient characteristics of the plate under investigation. A singularity will exist in numerical computation when r tends to zero; so to avoid singularity, we suppose a solid circular plate of non-dimensional radius$c$ at the center of the plate. Because of continuity conditions at the center of the circular plate, it is concluded that G is finite, thus the non-dimensional boundary conditions have the following forms at $r=c$:

$$G_{,r}=0,\quad G_{,rrr}=-\frac{1}{c}(G_{,rr})-\left(\frac{1-v^2}{h^3R}\right)\left(\frac{Qc}{2}\right),\quad F_{,r}=\frac{v}{c}F. \tag{45}$$

Moreover the circular plate edge is clamped at $r=1$, so the boundary conditions can be expressed as

$$G=0,\quad G_{,r}=0,\quad F_{,r}=vF. \tag{46}$$

3.2. Shooting method

When ordinary differential equations are required to satisfy boundary conditions at more than one value of the independent variable, the resulting problem is called a two-point boundary value problem. It is difficult to obtain analytical solutions of the nonlinear boundary-value problem of Eqs. (40) and (44); so to get a numerical solution of the problem, a shooting method or trial and error method [29,30] is employed. Differential equations of order higher than first can be written as coupled set of first-order, nonlinear ordinary differential equations as follows:

$$\frac{\mathrm{d}\mathbf{Y}}{\mathrm{d}r}=\mathbf{H}(r,\mathbf{Y};Q),\quad (c<r<1), \tag{47}$$

$$\mathbf{B}_1\mathbf{Y}(c)=\left\{\begin{array}{cccc} G(c) & 0 & -\left(\frac{1-v^2}{h^3R}\right)\left(\frac{Q}{2}\right)c & 0\end{array}\right\}^{\mathrm{T}},\quad \mathbf{B}_2\mathbf{Y}(1)=\{0\quad 0\quad 0\}^{\mathrm{T}} \tag{48a, b}$$

with

$$\mathbf{Y}=\{y_1,y_2,y_3,y_4,y_5,y_6,y_7\}^{\mathrm{T}}=\{G,G_{,r},G_{,rr},G_{,rrr},F,F_{,r},\Omega^2\}^{\mathrm{T}}, \tag{49}$$

$$\mathbf{H}=\{G_{,r},G_{,rr},G_{,rrr},G_{,rrrr},F_{,r},F_{,rr},0\}^{\mathrm{T}}=\{y_2,y_3,y_4,y_{4,r},y_6,y_{6,r},0\}^{\mathrm{T}}, \tag{50}$$

$$y_{4,r} = -\frac{2}{r}y_4 + \frac{1}{r^2}y_3 - \frac{1}{r^3}y_2 - \left(\frac{A(1-v^2)}{h^3B^2 - Ah^3R}\right) \times \left[\frac{3}{4r}(y_2y_6 + y_3y_5) + h\left(\frac{\rho_{cm}}{n+1} + 1\right)\Omega^2 y_1 + \left(\frac{h^3B}{1-v^2}\right)y_3^2 + Q\right], \tag{51}$$

$$y_{6,r} = -\frac{1}{r}y_6 + \frac{1}{r^2}y_5 - \left(\frac{hA}{2r}\right)y_2^2, \tag{52}$$

$$\mathbf{B}_1 = \begin{bmatrix} 1 & 0 & 0 & 0 & 0 & 0 & 0 \\ 0 & 1 & 0 & 0 & 0 & 0 & 0 \\ 0 & 0 & 1/c & 1 & 0 & 0 & 0 \\ 0 & 0 & 0 & 0 & -v/c & 1 & 0 \end{bmatrix}, \quad \mathbf{B}_2 = \begin{bmatrix} 1 & 0 & 0 & 0 & 0 & 0 & 0 \\ 0 & 1 & 0 & 0 & 0 & 0 & 0 \\ 0 & 0 & 0 & 0 & -v & 1 & 0 \end{bmatrix}. \tag{53}$$

By considering the initial-value problem corresponding to the boundary-value problem (47) and (48)

$$\frac{\mathrm{d}\mathbf{Z}}{\mathrm{d}r} = \mathbf{H}(r, \mathbf{Z}; Q), \quad r > c, \tag{54}$$

$$\mathbf{Z}(c) = \mathbf{I}(G(c), \mathbf{U}) = \left\{ G(c) \quad 0 \quad u_1 \quad -\left(\frac{1-v^2}{h^3R}\right)\left(\frac{Q}{2}\right)c - \frac{u_1}{c} \quad u_2 \quad \frac{vu_2}{c} \quad u_3 \right\}^{\mathrm{T}} \tag{55}$$

with

$$\mathbf{Z} = \{z_1, z_2, z_3, z_4, z_5, z_6, z_7\}^{\mathrm{T}}, \quad \mathbf{U} = \{u_1, u_2, u_3\}^{\mathrm{T}}, \tag{56}$$

where $\mathbf{U}$ is an unknown vector, relates to the missing initial values of $\mathbf{Y}$ at $x = c$. A solution of initial value problem (54) and (55) can be expressed as

$$\mathbf{Z}(r; G(c), \mathbf{U}, Q) = \mathbf{I}(G(c), \mathbf{U}) + \int_c^r \mathbf{H}(\zeta, \mathbf{Z}; Q)\,\mathrm{d}\zeta. \tag{57}$$

For a prescribed value of $G(c)$, the components of $\mathbf{U}$ are searched for such that solution (57), also satisfies boundary condition (48b), i.e.

$$\mathbf{B}_2\mathbf{Z}(1; G(c), \mathbf{U}^*, Q) = \{0 \quad 0 \quad 0\}^{\mathrm{T}}. \tag{58}$$

If $\mathbf{U} = \mathbf{U}^*$ is a root of Eq. (58), the solution for the boundary-value problem (47) and (48) is then obtained as

$$\mathbf{Y}(r) = \mathbf{Z}(r; G(c), \mathbf{U}^*, Q). \tag{59}$$

By employing a fourth-order Runge–Kutta method with variable steps to integrate Eq. (57) and at the same time, by using the Newton–Raphson method to find the root $\mathbf{U}^*$of algebraic Eq. (58), numerical solutions of Eqs. (47) and (48) have been obtained. If one obtains the solutions of Eqs. (47) and (48) for a sufficiently small value of dimensionless deflection parameter, then the solutions of Eqs. (40), (44)–(46) can be obtained for large scale of dimensionless deflection parameter by using the method of analytical continuation [1]. Therefore, a harmonic response of Eqs. (40), (44)–(46) is obtained in the form of Eqs. (38) and (39). Throughout the following numerical computation at uniform ambient temperature ($T = 300\,\mathrm{K}$), let $h/a = 0.04$, and $v = 0.28$. A relative error limit, $\varepsilon_1 = 10^{-6}$ was taken to warrant that both the numerical integration and the successive correction were carried out until the error norm became less than ε_1. When non-dimensional radius c tends to be zero, a singularity will exist in numerical computation; so we set $c = 0.0001$ approximately to take the place of the solid circular plate.

Table 2
Frequency ratio $\omega_{b1-NL}/\omega_{b1-L}$ for various non-dimensional vibration amplitudes associated with the first mode shape of clamped circular metallic plate for a Poisson's ratio $v = 0.3$

w_0/h	Present	[3]	[33]	[34]	[35]	[2]	[36]
0.2	1.0075	1.0072	1.0070	1.0079	1.0070	1.0075	1.0066
0.4	1.0296	1.0284	1.0278	1.0313	1.0278	1.0296	1.0263
0.5	1.0459	1.0439	1.0431	1.0485	1.0431	1.0459	1.0408
0.6	1.0654	1.0623	1.0614	1.0690	1.0614	1.0654	1.0583
0.8	1.1135	1.1073	1.1065	1.1194	1.1065	1.1135	1.1015
1.0	1.1724	1.1615	1.1617	1.1808	1.1617	1.1724	1.1547
1.5	1.3567	1.3255	1.3343	1.3711	1.3343	1.3568	1.3229
2.0	1.5789	1.5147	1.5423	1.5982	1.5424	1.5790	1.5275

Table 3
Computed values of the normalized linear and nonlinear fundamental mode shape ($G(r)/G(c)$)

r^*	Initial-value method			
	$\omega = 10.216$ (linear)		$\omega = 16.125$ (nonlinear)	
	[1]	Present	[1]	Present
0.0	1.0000	1.0000	1.0000	1.0000
0.1	0.9773	0.9773	0.9820	0.9821
0.2	0.9122	0.9122	0.9289	0.9308
0.3	0.8073	0.8073	0.8426	0.8465
0.4	0.6746	0.6746	0.7272	0.7310
0.5	0.5246	0.5246	0.5887	0.5923
0.6	0.3708	0.3708	0.4364	0.4393
0.7	0.2275	0.2275	0.2826	0.2848
0.8	0.1091	0.1091	0.1438	0.1451
0.9	0.0291	0.0291	0.0410	0.0416
1.0	0.0000	0.0000	0.0000	0.0000

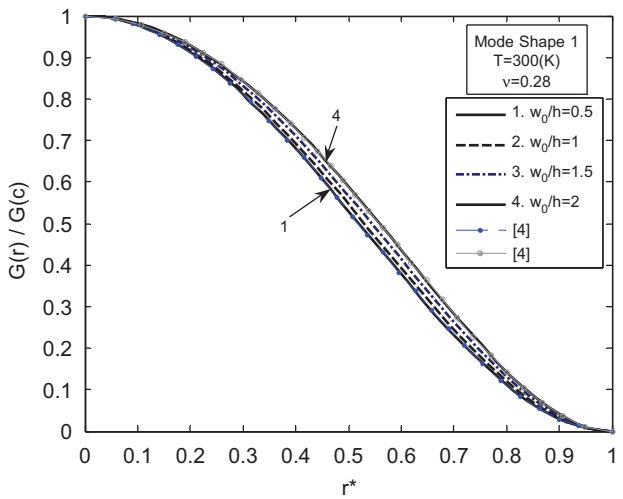

Fig. 3. Normalized nonlinear fundamental mode shape $G(r)/G(c)$ of a clamped immovable circular metallic plate for various non-dimensional central amplitudes of axisymmetric vibration.

3.3. Verification of solution approach

In order to show the reliability of the numerical technique employed here, we firstly give some numerical tests. The present results are validated by considering the linear and nonlinear steady-state free and forced vibration of a clamped circular metallic ($n \gg 100$) plate.

Non-dimensional linear natural frequencies of clamped circular plates are given by [1,16,31,32]

$$\omega_{bi} = a^2\Omega_i/h\sqrt{12\rho_m(1-\nu^2)/E_m}. \tag{60}$$

For linear axisymmetric vibration (the case of zero nodal diameters) of a clamped circular isotropic plate, the first four non-dimensional linear natural frequencies are [31]

$$\omega_{b1} = 10.216, \quad \omega_{b2} = 39.771, \quad \omega_{b3} = 89.104, \quad \omega_{b4} = 158.181. \tag{61}$$

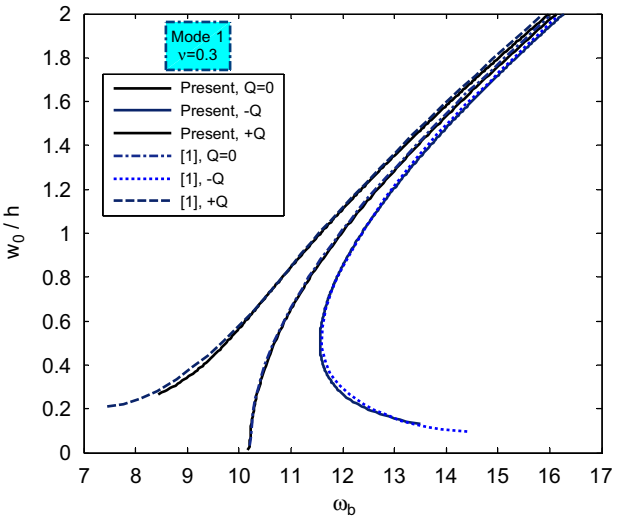

Fig. 4. Harmonic response of the clamped circular metallic plate around the first mode for the uniformly distributed load ($Q = 1.5 \times 10^{-9}$), values taken from Ref. [1], read from graph.

Table 4
Variation of the first two non-dimensional linear natural frequencies of axisymmetric vibration of the clamped circular functionally graded plate for different values of n at $\nu = 0.28$ and $T = 300\,\mathrm{K}$

n	$w_0/h = 0.0025$	$w_0/h = 0.00025$
	ω_{b1}	ω_{b2}
Ceramic	23.5873	–
0.01	23.2964	–
0.1	21.2723	82.8410
0.5	17.2985	67.0527
0.8	16.0439	62.0397
1	15.4879	59.8276
5	12.4211	48.1363
10	11.5676	45.0113
100	10.3896	40.4821
1000	10.2338	39.8233
10000	10.2176	39.7968
Metal	10.2160	39.7710

According to the vibration mode, ω_{bi} is the beginning point in the amplitude–frequency figures for linear free vibrations.

Firstly, the present numerical method is validated by considering the linear free vibration of a circular metallic plate with clamped immovable edge for prescribed values of $a/h = 136.59$ and $\nu = 0.3$. The maximum non-dimensional amplitude obtained at the plate center is w_0/h, and the ratio of the non-dimensional nonlinear frequency to the corresponding non-dimensional linear frequency is $\omega_{b-NL}/\omega_{b-L}$. Table 2 summarizes a set of results which are based on various solution techniques. Effects of large vibration amplitudes on the frequency ratio ($\omega_{b1-NL}/\omega_{b1-L}$) of the first nonlinear, axisymmetric mode shape and hardening spring effect are shown in Table 2. It can be seen also that the present results are very close to those of Ref. [2].

Secondly, for linear and nonlinear free vibration at the first mode, the computed values of the normalized mode shape ($G(r)/G(c)$) along the dimensionless radius are presented in Table 3. Good agreements can be seen between the results. In Fig. 3, nonlinear normalized fundamental mode shapes $G(r)/G(c)$ of a clamped immovable circular metallic plate for various non-dimensional amplitudes of axisymmetric vibration are plotted. The results are in good agreement with those given in Ref. [4].

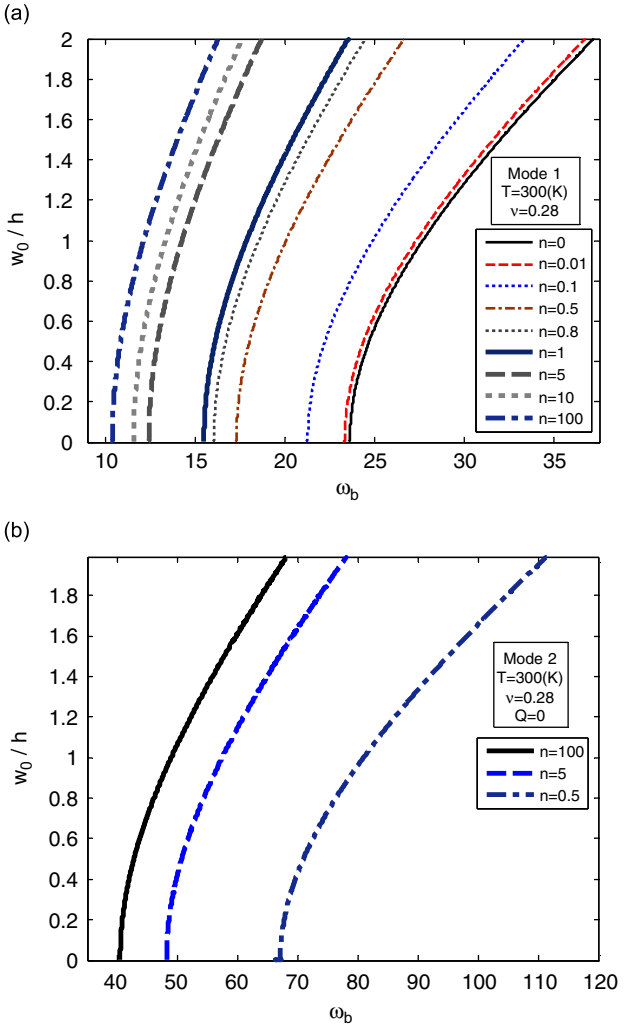

Fig. 5. Variation of the first (a) and second (b) non-dimensional natural frequencies of the clamped circular functionally graded plate with dimensionless central amplitudes of axisymmetric vibration.

Thirdly, Fig. 4 focuses on the harmonic response of the clamped circular metallic plate in transverse vibration. This figure describes the jump phenomenon and also the influence of amplitude on the non-dimensional linear and nonlinear frequencies (ω_b) of metallic plate in free ($Q=0$) and forced ($Q=1.5\times10^{-9}$) vibration around the first mode. The dimensionless, nonlinear frequencies of Ref. [1] were read from graph. The close agreement between the results of this study and the results of Ref. [1] is observed.

Based on the numerical comparison studies, we can confirm that the present numerical study can yield accurate solutions.

4. Numerical results and discussions

Some numerical examples are now demonstrated for the clamped circular functionally graded plate. Variation of the first non-dimensional linear and nonlinear natural frequencies with dimensionless central amplitudes of axisymmetric vibration for different values of n, are shown in Table 4 and Fig. 5(a), respectively. Volume fraction of metallic phase increases by increasing n. From Eq. (60), excellent agreement can be seen between ω_{b1} and the first non-dimensional linear natural frequency which is obtained for $n\gg100$. It is clear

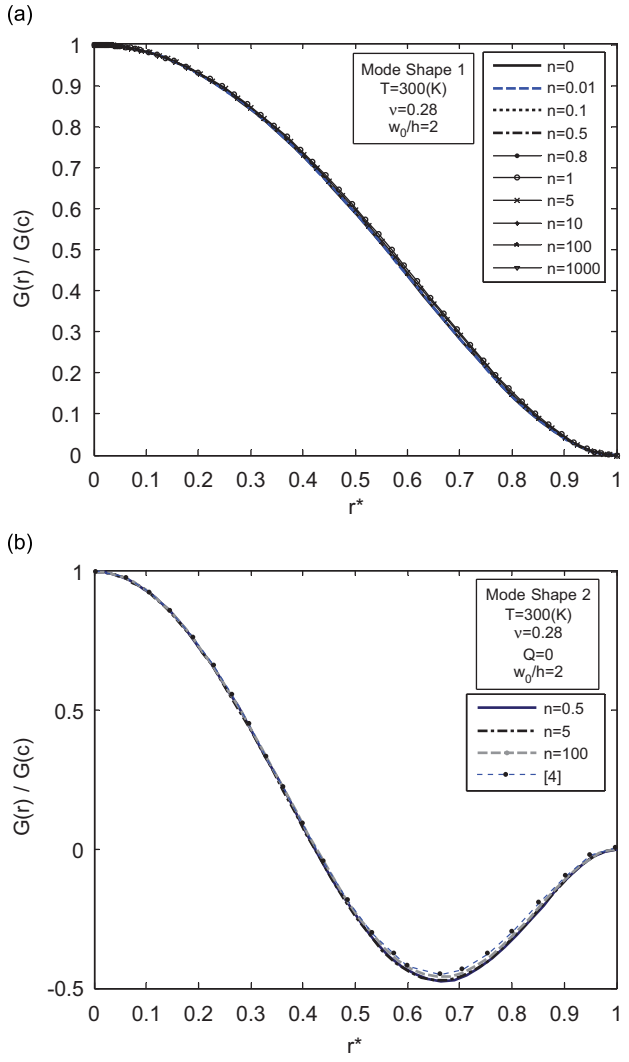

Fig. 6. First (a) and second (b) nonlinear normalized axisymmetric mode shapes of the clamped circular functionally graded plate for different values of n.

from Figs. 1 and 2 and Eq. (60) that, by increasing n, dimensionless Young's modulus decreases and dimensionless mass density increases. Consequently, the fundamental natural frequency decreases. It is noted that the fundamental frequency of the plate increases with the amplitude of vibration. This is due to the fact that the in-plane forces in the plate contribute to the lateral stiffness resulting from nonlinear coupling. A hardening type of nonlinearity is observed in this figure. This indicates that the fundamental frequency depends upon the amplitude of vibration, which is significantly different from the linear dynamic response. Variation of the second non-dimensional natural frequency with dimensionless central amplitude for different values of$n$ is plotted in Fig. 5(b). By increasing n, the second natural frequency decreases. For $n \gg 100$, linear frequency will be approximately ω_{b2}.

The first and second nonlinear normalized axisymmetric mode shapes for various values of n at $w_0/h = 2$ are plotted in Figs. 6(a) and (b), respectively. We can see that in this case the influence of variation of n in the nonlinear fundamental mode shape is important in the central part of the plate. Also in Fig. 6(b), it can be seen that the results are in a good agreement near the clamped edge. However, some discrepancy is seen in the central part of the plate. In Fig. 6(b) for the second nonlinear axisymmetric mode shape and for $n \gg 100$, a comparison is made between the results obtained here and those obtained in Ref. [4]. The results show the good agreement. In Figs. 7(a) and (b), the nonlinear normalized mode shapes of the first two axisymmetric

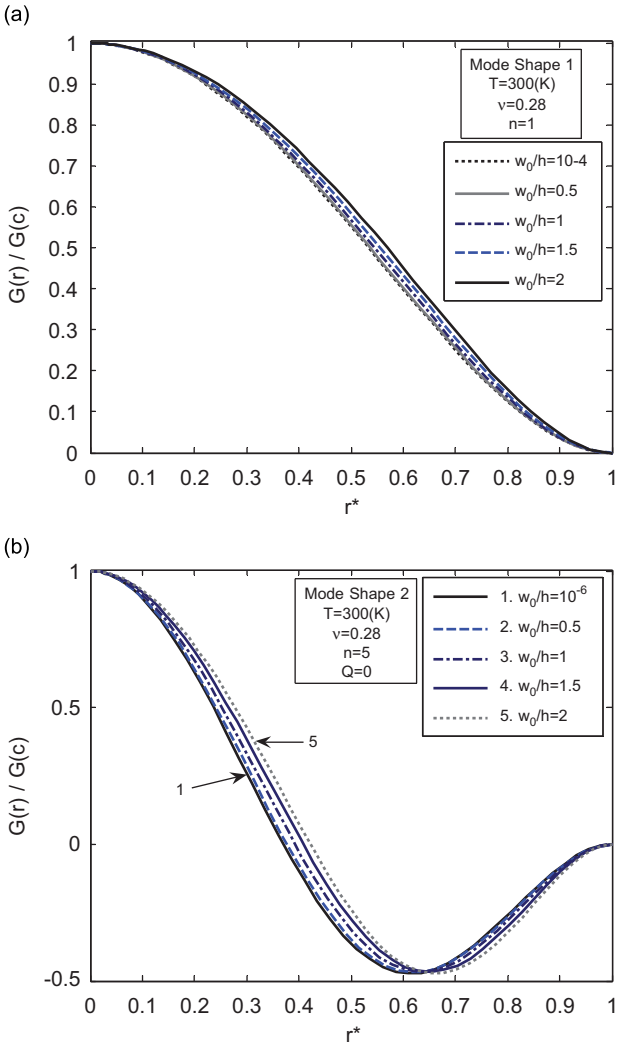

Fig. 7. Central amplitude dependent, normalized first (a) and second (b) mode shapes of the clamped circular functionally graded plate.

modes of a clamped, immovable, circular functionally graded plate are plotted, respectively, for various values of the non-dimensional amplitudes (w_0/h) of vibration at the center. The curves show that the curvatures near the clamped edge increase by increasing w_0/h. These results may lead one to expect that the bending stress near the edge of the plate will increase nonlinearly with the increase of the vibration amplitude. Fig. 8 indicates variations of the ratio of nonlinear to linear frequencies of the clamped circular functionally graded plate with dimensionless central amplitudes for the first and second axisymmetric mode shapes. In this figure, the first nonlinear mode shape exhibits less change in frequency with the vibration amplitude than does the second nonlinear axisymmetric mode shape, and it can be explained by the fact that the deflection shape, associated with the first mode shape, produces less induced tensile forces than does that associated with the second mode shape for the same maximum displacement amplitude. It can be observed that the results for $n \gg 100$ agree well with those of Ref. [4] which have been obtained for clamped immovable circular plate. Fig. 9 shows the relation of the central amplitude of axisymmetric vibration and the first non-dimensional natural frequencies for different values of Poisson's ratio v at $n = 0.5$. The first nonlinear normalized axisymmetric mode shape for

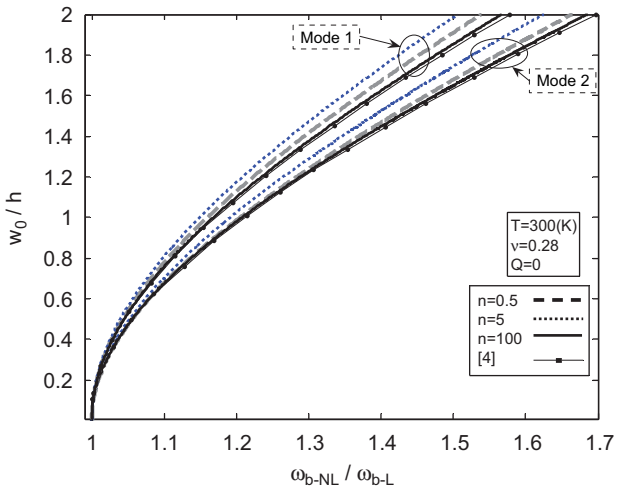

Fig. 8. Dependency of the ratio of nonlinear to linear frequencies of the clamped circular functionally graded plate with dimensionless central amplitudes for the first and second axisymmetric mode shapes and comparison with Ref. [4].

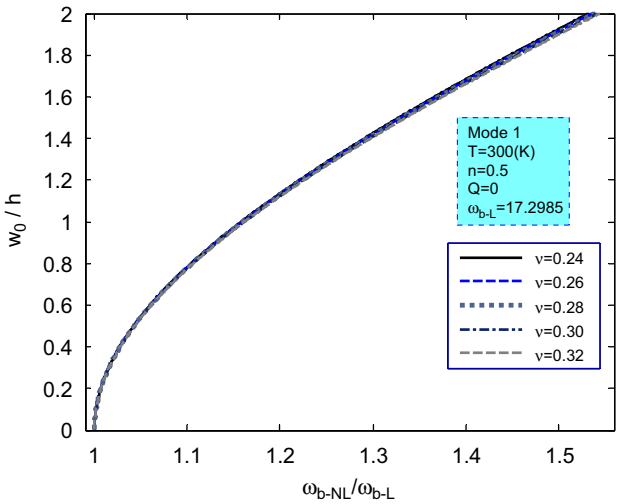

Fig. 9. Influence of different Poisson's ratio v on the fundamental non-dimensional natural frequencies.

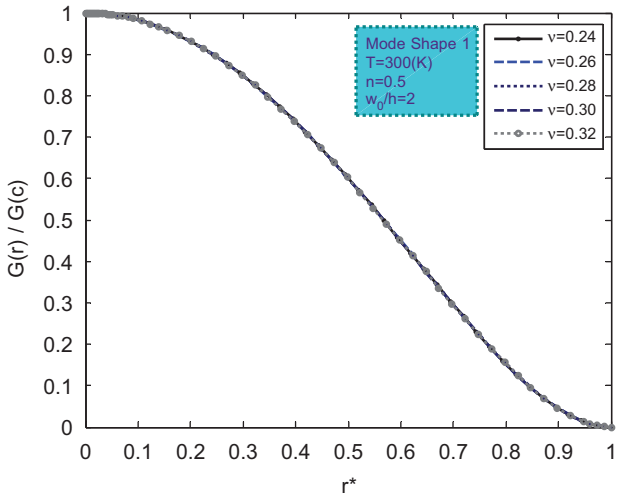

Fig. 10. First nonlinear normalized axisymmetric mode shape of the clamped circular functionally graded plate for different values of Poisson's ratio v.

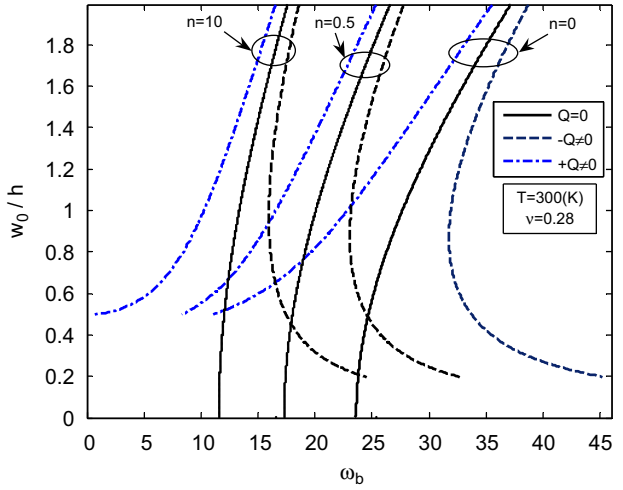

Fig. 11. Free ($Q=0$) and forced ($Q=10^{-5}$) harmonic response of the clamped circular functionally graded plate for the uniformly distributed load around the first mode.

the same conditions at $w_0/h=2$ is shown in Fig. 10. The results indicate that, for a clamped circular plate, the influence of Poisson's ratio on the fundamental frequencies is negligible; so we have used the average Poisson's ratio ($v=0.28$) in this paper.

Fig. 11 illustrates free ($Q=0$) and forced ($Q=10^{-5}$) harmonic vibration of the clamped circular functionally graded plate around the first mode for different values of n. In right branches of the mentioned figure, the points of vertical tangency give rise to a jump phenomenon commonly found in nonlinear vibratory systems.

Variation of the dimensionless radial total stress with dimensionless radius on metal-rich surface and non-dimensional radial total stress distribution along non-dimensional radius associated with the clamped immovable circular metallic plate for the first nonlinear axisymmetric mode shape have been presented in Ref. [37]. An excellent agreement between the results of this study and Ref. [4], for a metallic plate, can be seen.

5. Conclusions

The nonlinear free and forced vibration problems of a thin circular functionally graded plate have been investigated in this paper. The von-Karman's plate theory for large transverse deflections along with displacement field corresponding to the classical plate theory and a semi-analytical approach has been used. The FGM properties vary through the constant thickness of the plate. The results of this study in special cases were compared with the response of free and forced vibration of a clamped circular metallic plate in linear and nonlinear cases. In the results, the influences of vibration amplitude, variation of Poisson's ratio and volume fraction index have been examined. Several conclusions may be drawn from this study. It is considered that variation of volume fraction index is influential in FGM properties, dynamic treatment and the amount of stresses. The vibration frequencies are dependent on large vibration amplitudes, and for a clamped circular plate the effect of variation of Poisson's ratio on the fundamental frequencies is negligible.

References

[1] C.L. Huang, B.E. Sandman, Large amplitude vibrations of rigidly clamped circular plates, *International Journal of Nonlinear Mechanics* 6 (1971) 451–468.
[2] C.L.D. Huang, I.M. Al-Khattat, Finite amplitude vibrations of a circular plate, *International Journal of Nonlinear Mechanics* 12 (1977) 297–306.
[3] M. Haterbouch, R. Benamar, The effects of large vibration amplitudes on the axisymmetric mode shapes and natural frequencies of clamped thin isotropic circular plates, part I: iterative and explicit analytical solution for non-linear transverse vibrations, *Journal of Sound and Vibration* 265 (2003) 123–154.
[4] M. Haterbouch, R. Benamar, The effects of large vibration amplitudes on the axisymmetric mode shapes and natural frequencies of clamped thin isotropic circular plates, part II: iterative and explicit analytical solution for non-linear coupled transverse and in-plane vibrations, *Journal of Sound and Vibration* 277 (2004) 1–30.
[5] G.N. Praveen, J.N. Reddy, Nonlinear transient thermo elastic analysis of functionally graded ceramic-metal plates, *International Journal of Solids and Structures* 35 (1998) 4457–4476.
[6] J. Yang, H.S. Shen, Dynamic response of initially stressed functionally graded rectangular thin plates, *Composite Structures* 54 (2001) 497–508.
[7] J. Yang, H.S. Shen, Vibration characteristics and transient response of shear-deformable functionally graded plates in thermal environments, *Journal of Sound and Vibration* 255 (2002) 579–602.
[8] X.-L. Huang, H.-S. Shen, Nonlinear vibration and dynamic response of functionally graded plates in thermal environment, *International Journal of Solids and Structures* 41 (9–10) (2004) 2403–2427.
[9] J.N. Reddy, Z.Q. Cheng, Frequency of functionally graded plates with three-dimensional asymptotic approach, *Journal of Engineering Mechanics* 129 (2003) 896–900.
[10] J. Woo, S.A. Meguid, Nonlinear analysis of functionally graded plates and shallow shells, *International Journal of Solids and Structures* 38 (2001) 7409–7421.
[11] J. Woo, S.A. Meguid, L.S. Ong, Nonlinear free vibration behavior of functionally graded plates, *Journal of Sound and Vibration* 289 (3) (2006) 595–611.
[12] S. Kitipornchai, J. Yang, K.M. Liew, Semi-analytical solution for nonlinear vibration of laminated FGM plates with geometric imperfections, *International Journal of Solids and Structures* 41 (2004) 2235–2257.
[13] S. Kitipornchai, J. Yang, K.M. Liew, Random vibration of the functionally graded laminates in thermal environments, *Computer Methods in Applied Mechanics and Engineering* 195 (9–12) (2006) 1075–1095.
[14] J. Yang, S. Kitipornchai, K.M. Liew, Large amplitude vibration of thermo-electro-mechanically stressed FGM laminated plates, *Computer Methods in Applied Mechanics and Engineering* 192 (35–36) (2003) 3861–3885.
[15] Z.H. Guo, *Nonlinear Elasticity*, Science Press, Beijing, 1980.
[16] C.Y. Chia, *Nonlinear Analysis of Plates*, McGraw-Hill, New York, 1980.
[17] Y.S. Touloukian, *Thermo Physical Properties of High-Temperature Solid Materials*, Macmillan, New York, 1967.
[18] J.N. Reddy, C.D. Chin, Thermo-mechanical analysis of functionally graded cylinders and plates, *Journal of Thermal Stresses* 21 (1998) 593–626.
[19] J.N. Reddy, Analysis of functionally graded plates, *International Journal for Numerical Methods in Engineering* 47 (2000) 663–684.
[20] H. Shafiee, M.H. Naei, M.R. Eslami, In-plane and out-of-plane buckling of arches made of FGM, *International Journal of Mechanical Sciences* 48 (2006) 907–915.
[21] D.O. Brush, B.O. Almroth, *Buckling of Bars, Plates and Shells*, McGraw-Hill, New York, 1975.
[22] M.M. Najafizadeh, M.R. Eslami, Buckling analysis of circular plates of functionally graded materials under uniform radial compression, *International Journal of Mechanical Sciences* 44 (2002) 2479–2493.
[23] S. Timoshenko, J.N. Goodier, *Theory of Elasticity*, McGraw-Hill, New York, 1951.
[24] S. Timoshenko, S. Woinowsky-Krieger, *Theory of Plates and Shells*, second ed., McGraw-Hill, New York, 1959.

[25] S.-R. Li, Y.-H. Zhou, Shooting method for non-linear vibration and buckling of heated orthotropic circular plates, *Journal of Sound and Vibration* 248 (2001) 379–386.
[26] S.-R. Li, Y.-H. Zhou, Nonlinear vibration of heated orthotropic annular plates with immovably hinged edges, *Journal of Thermal Stresses* 26 (2003) 691–700.
[27] S.-R. Li, Y.-H. Zhou, X. Song, Nonlinear vibration and thermal buckling of an orthotropic annular plate with a centric rigid mass, *Journal of Sound and Vibration* 251 (2002) 141–152.
[28] P.C. Dumir, C.R. Kumar, M.L. Gandhi, Non-linear axisymmetric vibration of orthotropic thin circular plates on elastic foundations, *Journal of Sound and Vibration* 103 (1985) 273–285.
[29] L.S. Ma, T.J. Wang, Nonlinear bending and post-buckling of a functionally graded circular plate under mechanical and thermal loadings, *International Journal of Solids and Structures* 40 (2003) 3311–3330.
[30] H.P. William, P.F. Brain, A.T. Sau, *Numerical Recipes—The Art of Scientific Computing*, Cambridge University Press, New York, 1986.
[31] J.S. Rao, *Dynamics of Plates*, Narosa Publishing House, 1999.
[32] L. Meirovitch, *Principles and Techniques of Vibrations*, Prentice-Hall, Englewood Cliffs, NJ, 1997.
[33] N. Yamaki, Influence of large amplitudes on flexural vibrations of elastic plates, *Zeitschrift fur Angewandte Mathematik und Mechanik* 41 (1961) 501–510.
[34] J.L. Nowinski, Non-linear transverse vibrations of circular elastic plates built-in at the boundary, *Proceedings of the Fourth US National Congress on Applied Mechanics*, Vol. 1, 1962, pp. 325–334.
[35] G.C. Kung, Y.H. Pao, Non-linear flexural vibrations of a clamped circular plate, *Journal of Applied Mechanics, Transactions of the American Society of Mechanical Engineers* 39 (1972) 1050–1054.
[36] J. Ramachandran, Frequency analysis of plates vibrating at large amplitudes, *Journal of Sound and Vibration* 51 (1) (1977) 1–5.
[37] A. Allahverdizadeh, M.H. Naei, A. Rastgo, The effects of large vibration amplitudes on the stresses of thin circular functionally graded plates, *International Journal of Mechanics and Material in Design* 3 (2006) 161–174.